Biomedicine & Pharmacotherapy 138 (2021) 111501

Contents lists available at ScienceDirect

Biomedicine & Pharmacotherapy

journal homepage: www.elsevier.com/locate/biopha

Original article

Ex vivo and in vivo chemoprotective activity and potential mechanism of Martynoside against 5-fluorouracil-induced bone marrow cytotoxicity

Mengying Hong [a], Dongdong Chen [a], Zhuping Hong [b], Kejun Tang [a], Yuanyuan Yao [c], Liubo Chen [a], Tingting Ye [b], Jing Qian [b], Yushen Du [a,d,*], Ren Sun [a,d,e,*]

[a] Cancer Institute, The Second Affiliated Hospital, ZJU-UCLA Joint Center for Medical Education and Research, Zhejiang University School of Medicine, Hangzhou, Zhejiang 310009, China
[b] Pharmaceutical Informatics Institute, College of Pharmaceutical Sciences, Zhejiang University, Hangzhou 310058, Zhejiang Province, China
[c] Department of Colorectal Surgery, The First Affiliated Hospital, Zhejiang University School of Medicine, Hangzhou 310003, Zhejiang Province, China
[d] Department of Molecular and Medical Pharmacology, David Geffen School of Medicine, University of California at Los Angeles, Los Angeles, CA 90095, USA
[e] School of Biomedical Sciences, Li Ka Shing Faculty of Medicine, The University of Hong Kong, Hong Kong, China

ARTICLE INFO

Keywords:
Martynoside
5-fluorouracil
Bone marrow cytotoxicity
Chemoprotective activity
mRNA-Seq

ABSTRACT

Martynoside (MAR) is a bioactive glycoside of *Rehmannia glutinosa*, a traditional Chinese herb frequently prescribed for treating chemotherapy-induced pancytopenia. Despite its clinical usage in China for thousands of years, the mechanism of MAR's hematopoietic activity and its impact on chemotherapy-induced antitumor activity are still unclear. Here, we showed that MAR protected *ex vivo* bone marrow cells from 5-fluorouracil (5-FU)-induced cell death and inflammation response by down-regulating the TNF signaling pathway, in which Il1b was the most regulatory gene. Besides, using mouse models with melanoma and colon cancer, we further demonstrated that MAR had protective effects against 5-FU-induced myelosuppression in mice without compromising its antitumor activity. Our results showed that MAR increased the number of bone marrow nucleated cells (BMNCs) and the percentage of leukocyte and granulocytic populations in 5-FU-induced myelosuppressive mice, accompanied by an increase in numbers of circulating white blood cells and platelets. The transcriptome profile of BMNCs further showed that the mode of action of MAR might be associated with the increased survival of BMNCs and the improvement of the bone marrow microenvironment. In summary, we revealed the potential molecular mechanism of MAR to counteract 5-FU-induced bone marrow cytotoxicity both *ex vivo* and *in vivo*, and highlighted its potential clinical usage in cancer patients experiencing chemotherapy-induced multi-lineage myelosuppression.

1. Introduction

5-Fluorouracil (5-FU) is one of the most frequently used chemotherapeutic drugs for the treatment of solid tumors [1,2]. However, as the cell-killing mechanism is not tumor-specific, 5-FU may lead to severe side effects such as myelotoxicity. Manifested with neutropenia, thrombocytopenia, and anemia, myelotoxicity is the primary dose-limiting cytotoxicity when 5-FU is given as an intravenous bolus [3,4]. Mild myelosuppression can lead to dose reductions and treatment delays, while severe myelosuppression causes death-threatening complications such as fatal infections and uncontrollable bleeding.

Chinese herbal medications have historical therapeutic applications and are important sources of new drugs [5,6]. Besides, various plant-derived compounds have been found to have hematopoietic properties for chemo-induced myelosuppression [7–9]. In Eastern Asian countries, multiple Chinese herbal medications have been practiced

Abbreviations: MAR, Martynoside; 5-FU, 5-fluorouracil; DMSO, Dimethyl sulfoxide; mRNA-Seq, mRNA sequencing; BMNCs, Bone marrow nucleated cells; BMSCs, Bone marrow stromal cells; BMCs, Bone marrow cells; HSCs, Hematopoietic stem cells; RT, Room temperature; PFA, Paraformaldehyde; GO, Gene ontology; PPI, Protein-protein interaction; WT, Wild type; DEGs, Differentially expressed genes; cDEGs, Co-regulated DEGs; MeV, Multiple Experiment Viewer; FC, Fold change; H&E, Hematoxylin and eosin; CBC, Complete blood count analysis; RBC, Red blood cells; WBC, White blood cells; PLT, Platelets; RT-qPCR, Reverse transcription-quantitative PCR; FPKM, Fragments per kilobase million.

* Corresponding authors at: Cancer Institute, The Second Affiliated Hospital, ZJU-UCLA Joint Center for Medical Education and Research, Zhejiang University School of Medicine, Hangzhou, Zhejiang 310009, China.
E-mail addresses: lilyduyushen@zju.edu.cn (Y. Du), rensun@hku.hk (R. Sun).

https://doi.org/10.1016/j.biopha.2021.111501
Received 15 January 2021; Received in revised form 3 March 2021; Accepted 9 March 2021
Available online 23 March 2021

clinically to alleviate chemotherapy-related myelosuppression [7,10–14], such as *Ginseng*, *Herba Epimedii*, *Radix Sanguisorbae*. *Rehmannia glutinosa* is also widely utilized in multiple Chinese medicine prescriptions as a tonic for nourishing blood [15,16], such as Rehmannia Six Formula (Liuwei Dihuang Wan) [17], Siwu decoction [18], and Fufang Ejiao syrupy [10,19]. Martynoside (MAR), the active ingredient found in *Rehmannia* [20,21], is a phenylpropanoid glycosidic compound with several known pharmacological features, especially hematopoietic activity [19,22,23]. Previously, we found that the application of MAR could facilitate the proliferation of hematopoietic stem cells (HSCs) in 5-FU-induced myelosuppressive mice [19]. However, the therapeutic effects of MAR in 5-FU-induced pancytopenia need a further detailed investigation, and its impact on the antitumor activity of 5-FU remains unknown.

In this study, we described the *ex vivo* and *in vivo* chemoprotective activity of MAR against 5-FU-induced bone marrow cytotoxicity without compromising its antitumor activity. Applying mRNA sequencing technology (mRNA-Seq) and transcriptome-based data analysis, we further investigated the biological processes, molecular pathways, and regulatory genes involved in MAR's myeloprotection function, both *ex vivo* and *in vivo*.

2. Materials and methods

2.1. Chemicals

MAR (purity $\geq$ 95%) was purchased from BioBioPha Company (Yunnan, China), dissolved in dimethyl sulfoxide (DMSO) at 100 mg/ml and stored at − 20 °C. 5-FU and uridine were purchased from the Yuanye Bio-Technology Co., Ltd. (Shanghai, China) and Bide Pharmatech Ltd. (Shanghai, China), respectively. 50 μg/ml MAR, 12.5 μg/ml 5-FU, and 0.1 mM uridine were used in the cellular model.

2.2. Preparation of bone marrow nucleated cells

Bone marrow nucleated cells (BMNCs) and bone marrow stromal cells (BMSCs) were harvested as previously described [22]. Briefly, the femurs of the mice were taken out and soaked in α-MEM medium (Gibco) after the mice were sacrificed. A 1 ml syringe was used to flush bone marrow cells (BMCs) out with α-MEM medium. The BMNCs were obtained after erythroid bone marrow cells were lysed with ammonium chloride buffer (NH_4Cl). BMNCs were allowed to grow in cell culture plates for 24 h, and the adherent cells were taken as BMSCs. The primary cells were grown in α-MEM medium with 10% FBS (Gibco) and 100 U/ml of penicillin-streptomycin.

2.3. Cell viability staining

Dead cells were stained with fixable viability dye (Zombie Red™ Fixable Viability Kit). After finishing the indicated treatments, cells were washed and incubated with the fixable viability dye (1:300) at room temperature (RT) for 30 min in darkness. After washing, cells were fixed with freshly prepared 4% paraformaldehyde (PFA) at RT for 10–15 min. Then cells were permeabilized on ice with PBS/0.25% Triton X-100 for 10 min and counterstained with 2 μg/ml DAPI (Beyotime, Jiangsu, China).

2.4. Mouse experiments

Wild type (WT) female C57BL/6 mice at 7 weeks of age were purchased from the Shanghai Laboratory Animal Company (SLAC, Shanghai, China) and maintained at Zhejiang University Laboratory Animal Center. Mice experiments were performed in compliance with *the National Institutes of Health Guide for the Care and Use of Laboratory Animals*. A total of 5×10^5 B16-F10 melanoma cells and 2×10^6 MC38 colon cancer cells were injected subcutaneously (s.c.) into the right flank of mice and tumor growth was measured every other day. The following formula is used to calculate tumor volume.

$$Tumor\ \ Volume = 1/2\ \times\ (\text{length} \times \text{width}^{\,2})$$

Treatment was initiated when the tumor size reached around 200 mm^3. Mice were randomly selected and divided into four groups: the control group (CTR), MAR-only treatment group (MAR), 5-FU-only treatment group (5-FU), and combined treatment group (5-FU + MAR). 40 mg/kg 5-FU was administered intraperitoneally for 7 consecutive days to achieve a degree of peripheral blood abnormalities similar to cancer patients receiving 5-FU treatment [24]. MAR was administrated by oral gavage at a dosage of 20 mg/kg/d based on our previous study and reported literature [22,23]. Correspondingly, the control group received an equal volume of PBS. After finishing 7 consecutive days of treatment, the mice were anesthetized with 1.5% pentobarbital sodium and blood samples were collected with the cardiac puncture. Then the blood samples were stored in K2-EDTA tubes and analyzed in an automatic hematology analyzer (BC-2800vet, Wuhan Servicebio Technology, China). The femurs of mice from the different groups were put into 4% PFA, decalcified in EDTA solution, embedded in paraffin, and cut into slices. BMCs were collected from the medullary canal of the right femurs and tibias. Cells (1×10^5~1×10^6) were stained with Zombie, anti-CD11b, anti-CD45, and anti-Gr-1 antibodies. The percentages of leukocytes (CD45+) and granulocytes (CD11b+Gr-1+) in BMCs were calculated with flow cytometry. Besides, the number of BMNCs was calculated using a counting chamber. The excised tumor tissues were digested in a 37 °C water bath for 45 min at a collagenase A (Sigma) concentration of 1 mg/ml. The tumor cells were passed through 70 μM falcon strainers by gravity flow and lysed with ACK lysis buffer (Thermo Fisher Scientific). Tumor cells (5×10^5) were suspended with Zombie in 100 μl FACS buffer (PBS + 4% FBS) (1:400), fixed with 2% PFA at RT for 30 min, and incubated with anti-mouse CD45 antibody on ice for 30 min.

2.5. mRNA-Seq and data processing

BMSCs were treated with 0.1% DMSO (DMSO), 50 μg/ml MAR (MAR), 12.5 μg/ml 5-FU (5-FU), or 5-FU in combination with MAR (5-FU + MAR) for 48 h before total RNA was extracted. In the B16-F10 model, mRNA-Seq analysis was performed in BMNCs isolated from 2 randomly selected mice in the CTR, 5-FU, and 5-FU + MAR groups. The total RNA was purified with poly-T oligo attached magnetic beads. Then, purified mRNA was fragmented and reverse transcribed. The sequencing library was prepared and sequenced on the Illumina Novaseq platform. Finally, 150 bp paired-end reads were obtained. Trimmomatic v0.36 software was applied to obtain clean data by removing low-quality bases and adapters. Then clean data were aligned to the mouse reference genome (Mus_musculus.GRCm38.94.chr.gtf) using Hisat2 software. Then featureCounts software was used to generate gene counts. Differentially expressed genes (DEGs) of BMSCs and BMNCs are shown in Supplementary Table S1 and Supplementary Table S2, respectively.

2.6. Functional analysis

The functional analysis of mRNA-Seq data was based on DEGs. 5-FU and MAR co-regulated DEGs (cDEGs) were obtained by Venn diagrams using Venny 2.1.1. A hierarchically clustered heatmap was applied to compare the expression of cDEGs in 5-FU vs CTR and 5-FU + MAR vs 5-FU groups using Multiple Experiment Viewer (MeV). Gene ontology (GO) and KEGG pathway enrichment analysis were conducted using DAVID Bioinformatics Resources 6.8 and the P values < 0.05 were considered as statistically significant [25,26]. Protein-protein interaction (PPI) network was obtained and visualized with String and Cytoscape platforms [27,28]. Hub genes were identified using the CytoHubba plugin and the MCC calculation method [29]. Key

sub-networks were obtained using the MCODE plugin [30].

2.7. Flow cytometry

Flow cytometry was conducted on the BD LSRFortessa™ cell analyzer and Beckman Coulter's CytoFLEX cytometer on the Core facilities, School of medicine, Zhejiang University.

2.8. Reverse transcription-quantitative PCR analysis

Reverse transcription-quantitative PCR (RT-qPCR) was used to assess the gene expression of several inflammatory genes in BMSCs receiving different treatments and BMNCs obtained from different treatment groups. Total RNA was extracted with the Ultrapure RNA kit (CWBIO, Beijing, China) and reverse-transcribed with the HiFiScript cDNA Synthesis kit (CWBIO, Beijing, China). RT-qPCR was carried out on the

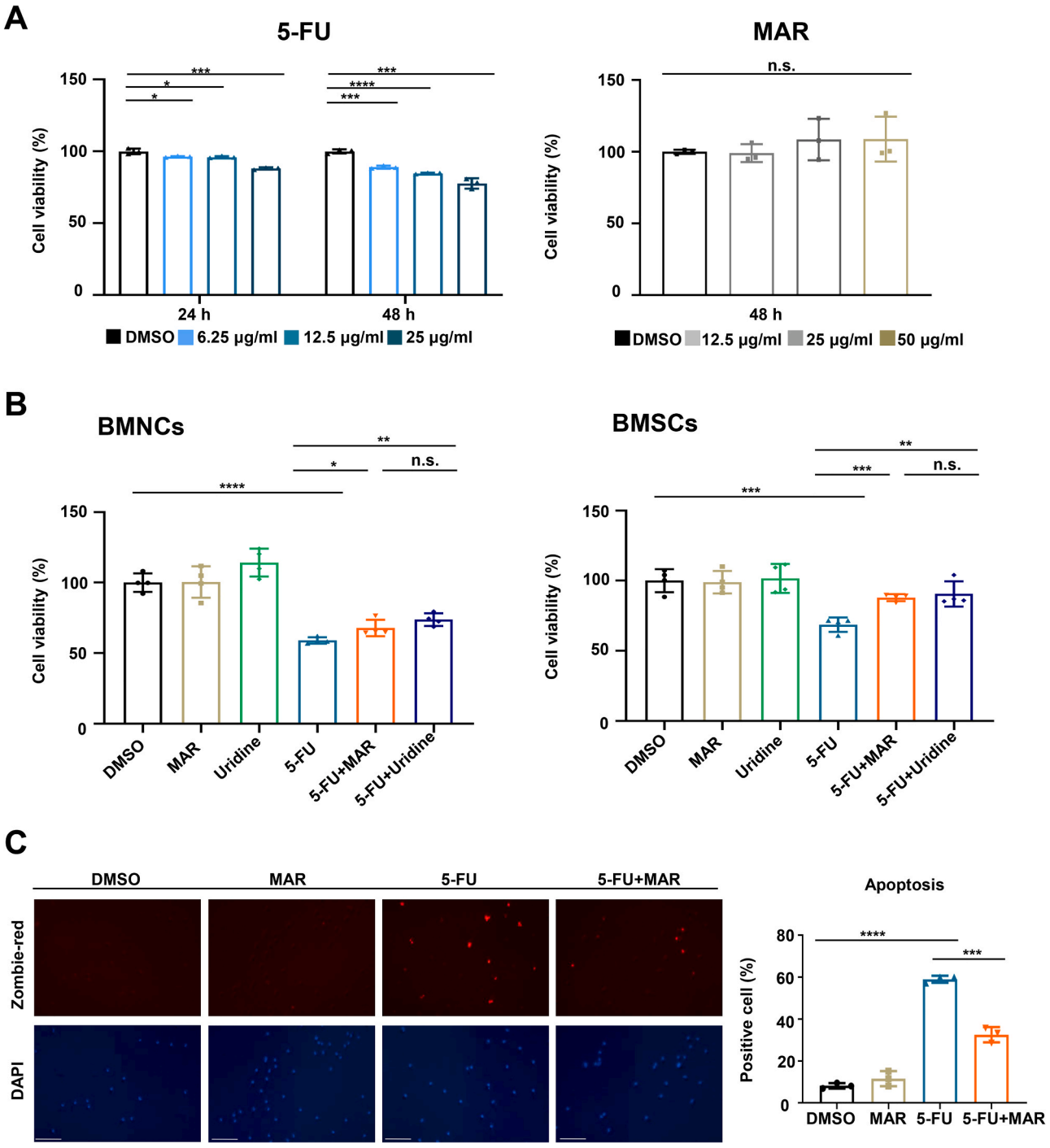

Fig. 1. MAR attenuates 5-FU-induced cytotoxicity in BMNCs and BMSCs *ex vivo*. (**A**) *Ex vivo* cytotoxicity of 5-FU and MAR in BMNCs. CCK-8 assay evaluated the toxicity effects of different concentrations of 5-FU and MAR for BMNCs. (n = 4 for 5-FU, n = 3 for MAR). (**B**) MAR increases the cell viability reduced by 5-FU in BMNCs and BMSCs. CCK-8 assay evaluated the effects of MAR (50 μg/ml) and uridine (0.1 mM) on 5-FU (12.5 μg/ml)-induced cytotoxicity for 48 h. (n = 4). (**C**) MAR reverses the pro-apoptotic effects of 5-FU in BMSCs. The dead cells were determined by zombie red staining in BMSCs after received 48 h of indicated treatment. Scale bar = 100 μm. The histogram shows the percentage of dead cells. (n = 3). All data are presented as mean ± SD. *P < 0.05, **P < 0.01, ***P < 0.001, ****P < 0.0001, n.s. = no significance. (For interpretation of the references to colour in this figure legend, the reader is referred to the web version of this article.)

CFX96 Touch Real-Time PCR system (Bio-Rad, Hercules, CA) using a 1X T5 fast qPCR mix (TsingKe, Hangzhou, China). GAPDH was used as an endogenous control. The relative expression was analyzed with the $2^{-\Delta\Delta CT}$ method and presented as the fold change (FC) relative to the control. The primer sequences that were synthesized by SunYa (Hangzhou, China) are listed in Supplementary Table S3.

2.9. Antibodies

The Zombie NIR™ fixable viability kit (423105), Zombie red fixable viability kit (423109), APC anti-mouse CD45 antibody (103112), PE anti-mouse Ly-6G/Ly-6C (Gr-1) (108407), and FITC anti-mouse/human CD11b antibody (101205) antibody were obtained from Biolegend (CA, USA).

2.10. Statistical analysis

Without specific notification, all statistical data are shown as means ± SD and the statistical significance analysis was performed by a two-tailed Student's *t*-test. The statistical significance and P value analysis were specified in each figure legend.

2.11. Data availability

The sequencing data have been deposited to the NCBI BioProject database, with the BioProject ID PRJNA616155.

3. Results

3.1. MAR enhances bone marrow nucleated cell viability exposed to 5-FU ex vivo

In this study, we first evaluated the effects of 5-FU and MAR on the cell viability of BMNCs, which were isolated from the bone marrow of WT C57BL/6 mice and cultured *ex vivo*. CCK-8 results showed that 5-FU significantly inhibited the cell viability of BMNCs in a dose- and time-dependent manner (P value < 0.05), while 50 μg/ml MAR showed no significant effects up to 48 h (P value > 0.05) (Fig. 1A). 12.5 μg/ml 5-FU treatment on BMNCs for 48 h, as the dose with mild but significant cytotoxicity compared with DMSO treatment (P value < 0.0001), was selected for the following experiments. We found that 5-FU caused a decrease in total cell number and cellular shrinkage of adherent BMSCs that could be partially reversed by additional MAR (Supplementary Fig. 1). Consistent with morphology, CCK-8 assay demonstrated that the reversal of 5-FU-induced BMNCs and BMSCs toxicity could be achieved by 50 μg/ml MAR (Fig. 1B). Notably, both in BMNCs and BMSCs, the *ex vivo* protective activity of MAR is comparable with 0.1 mM uridine, which is the reported antidote with an effective dose against 5-FU-induced bone marrow cytotoxicity [31,32]. Besides, viability staining of BMSCs with zombie dyes identified that the treatment of 5-FU significantly increased the percentage of apoptotic BMSCs to 60%, which was reduced to ~30% by the additional MAR (Fig. 1C). This data shows that the 5-FU-induced bone marrow nucleated cell cytotoxicity can be partially reversed by MAR, confirming the protective effects of MAR in this *ex vivo* myelosuppression model.

3.2. Identification and functional analysis of cDEGs from ex vivo mRNA-Seq data

In the above section, we also found that MAR had protective effects on BMSCs against 5-FU-induced cytotoxicity (Fig. 1B), indicating that MAR may play a role in the reconstruction of the hematopoietic microenvironment. To comprehensively analyze the chemoprotective effects of MAR in the hematopoietic microenvironment, we performed mRNA-Seq for *ex vivo* BMSCs that received different treatments. In this model, the number of identified DEGs (DESeq2 P value < 0.05 and $|\log2FC| > 0.0$) from different comparison groups was shown in Fig. 2A (Supplementary Table S1). We identified 2,410 DEGs upon 5-FU treatment for 48 h, 727 of which were up-regulated and 683 were down-regulated. As shown in Fig. 2B, MAR oppositely down-regulated 51 DEGs and up-regulated 18 DEGs in 5-FU-treated BMSCs. To determine the functional terms and pathways affected by MAR, we used DAVID to conduct GO and KEGG pathway enrichment analysis for 69 cDEGs in the 5-FU vs DMSO group and 5-FU + MAR vs 5-FU group. The 18 MAR oppositely up-regulated cDEGs were significantly enriched in two biological processes (P value < 0.05), which were "negative regulation of tumor necrosis factor production" and "response to peptide hormone" (Fig. 2C). Meanwhile, the 51 MAR down-regulated cDEGs were predicted to participate in three biological processes, including inflammatory response, response to lipopolysaccharide, and innate immune response process (Fig. 2D). The corresponding KEGG pathway enrichment analysis showed that the TNF signaling pathway, NF-kappa B signaling pathway, and NOD-like receptor signaling pathway were enriched (Fig. 2D). Notably, both MAR up- and down-regulated cDEGs are associated with TNF signaling pathway, suggesting that it may be the most relevant pathway response to additional MAR treatment in 5-FU-treated BMSCs. Besides, PPI network analysis of cDEGs was performed using String plugin in Cytoscape 3.6.1 (Fig. 2E). The up- and down-regulated genes were colored in red and blue, respectively. The cDEGs related to significantly enriched pathways and biological processes were marked separately (P value < 0.05). Notably, 5-FU elevated the expression of several inflammation-related genes, such as Fpr3, Fpr1, Irg1, Il1b, Tlr2, and Cxcl2. We found that additional MAR treatment significantly down-regulated the expression of these inflammatory genes. Using the CytoHubba plugin, the hub genes in the PPI network were analyzed using the MCC method. Among them, two apoptosis and inflammation-related genes Il1b and Tlr2 with the highest connectivity scores, were considered to be key regulatory genes (Fig. 2F). These results indicate that MAR is most likely to be involved in the regulation of inflammatory response and the production of tumor necrosis factor in the hematopoietic microenvironment to alleviate the hematopoietic function damaged by 5-FU, through the TNF pathway.

3.3. Administration of MAR does not compromise the antitumor activity of 5-FU in B16-F10 and MC38 tumor-bearing mice

In the above sections, we showed that MAR attenuated 5-FU-induced cell death and inflammation response through the downregulation of the TNF signaling pathway in primary BMSCs. This evidence provides a rationale for MAR's clinical use as an adjuvant medication to treat 5-FU-induced myelosuppression. However, one question that needs to be addressed is whether MAR can affect the antitumor effect of 5-FU. To further characterize the impact of MAR on 5-FU-induced antitumor activity and side effects of myelotoxicity *in vivo*, we employed two subcutaneous tumor models in WT C57BL/6 mice: a melanoma model (B16-F10) and a colon cancer model (MC38) (Fig. 3A and Fig. 4A). After the subcutaneous tumors were established (~200 mm^3), mice were randomly divided into four groups: the control group (CTR), MAR-only treatment group (MAR), 5-FU-only treatment group (5-FU), and combined treatment group (5-FU + MAR). As expected, the continuous administration of 5-FU significantly inhibited tumor growth in both B16-F10 and MC38 mouse models (Figs. 3, B–D and 4, B and C). Co-administration of MAR did not interfere with the *in vivo* antitumor activity of 5-FU in both two tumor models. Interestingly, MAR-alone treatment did not exhibit antitumor property in the immune-cold B16-F10 model but showed slight antitumor activity in the MC38 mouse model, which was probably due to the increased infiltration of leukocytes (CD45+) (Fig. 4D).

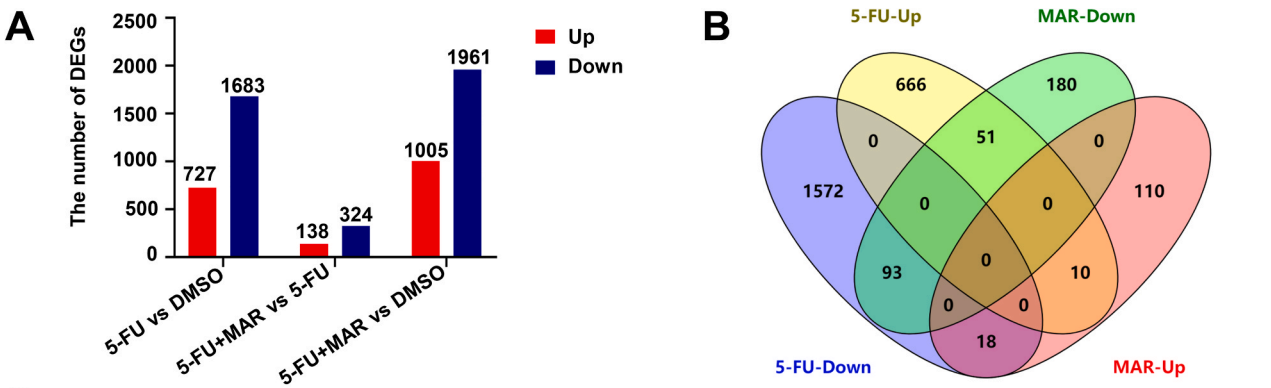

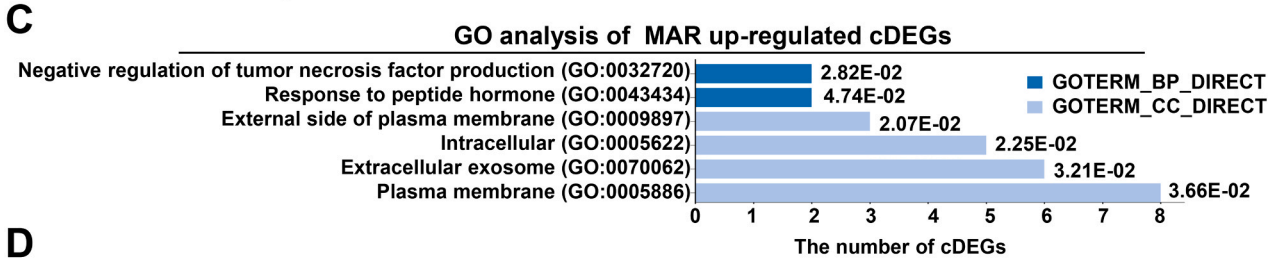

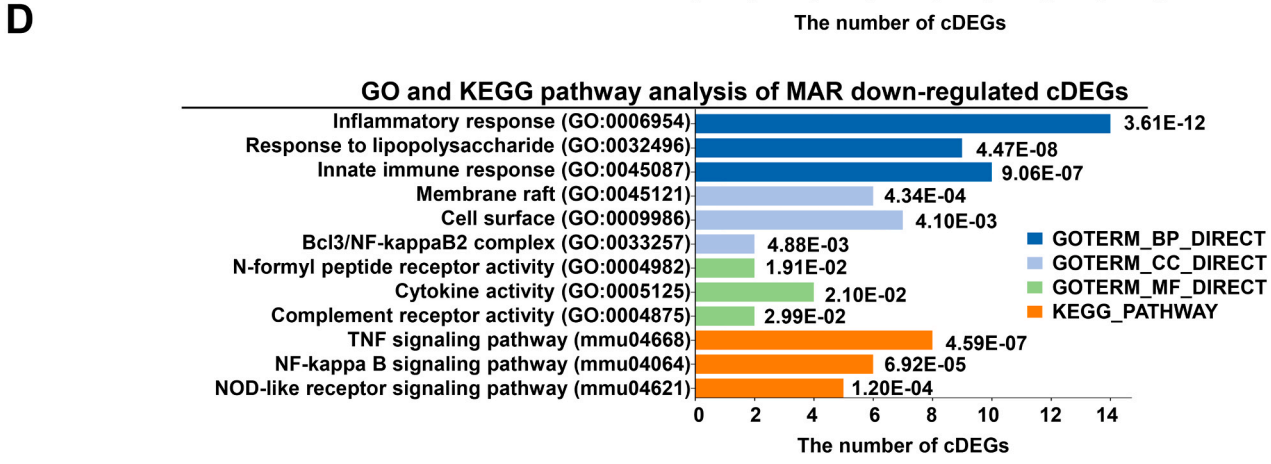

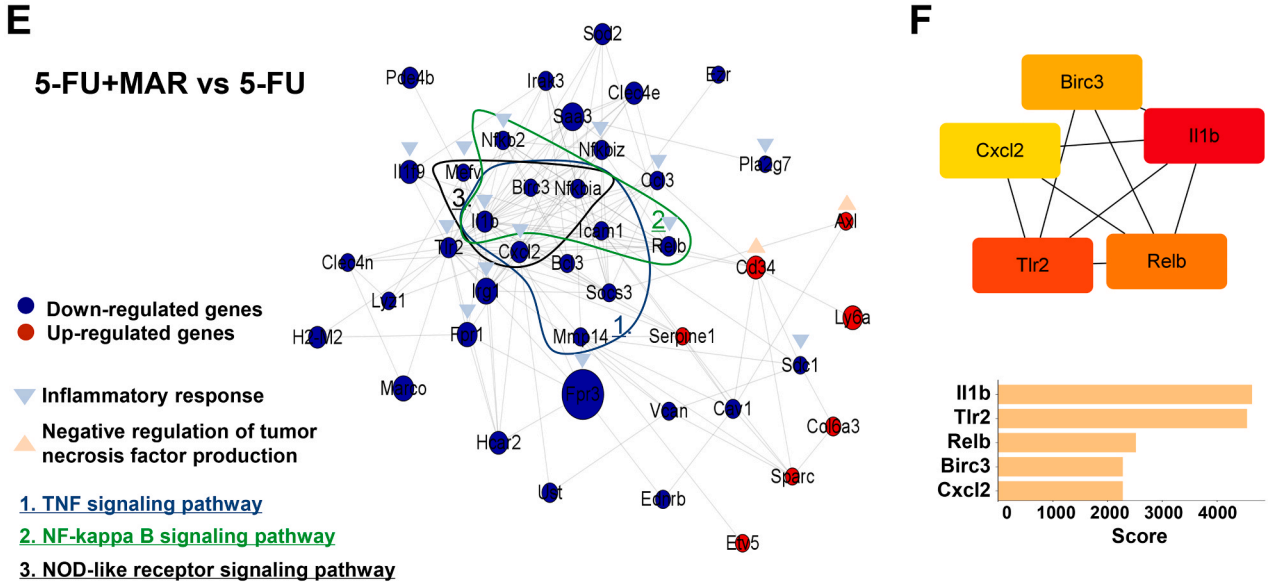

(caption on next page)

Fig. 2. cDEGs identification and functional analysis of BMSCs in the *ex vivo* myelosuppression model. (**A**) Number of up- and down-regulated DEGs. (**B**) Venn diagram showing the number of commonly and uniquely DEGs. The blue and yellow circles represent genes differentially down-regulated and up-regulated by 5-FU (vs DMSO), respectively. The green and pink circles represent genes differentially down-regulated and up-regulated by additional MAR (vs 5-FU), respectively. The numbers depicted at the intersection between the circles represent the counts of genes that are co-regulated by 5-FU and MAR. (**C**) Functional analysis of the 18 cDEGs up-regulated in the 5-FU-MAR vs 5-FU group and down-regulated in the 5-FU vs DMSO group. The GO terms are arranged by P value. (**D**) Functional analysis of the 51 cDEGs down-regulated in the 5-FU-MAR vs 5-FU group and up-regulated in the 5-FU vs DMSO group. The KEGG pathway terms are arranged by P value. (**E**) PPI network of cDEGs in the 5-FU-MAR vs 5-FU group. The size of each node denotes the absolute value of log2FC, and the color of the node represents the gene regulatory type. (**F**) PPI network analysis of the top 5 hub genes. The Cytoscape plugin CytoHubba and the MCC calculation method were used to identify the hub nodes. Warm color nodes share higher connectivity degrees. The order of genes is arranged in the order of connectivity score from high to low. (For interpretation of the references to colour in this figure legend, the reader is referred to the web version of this article.)

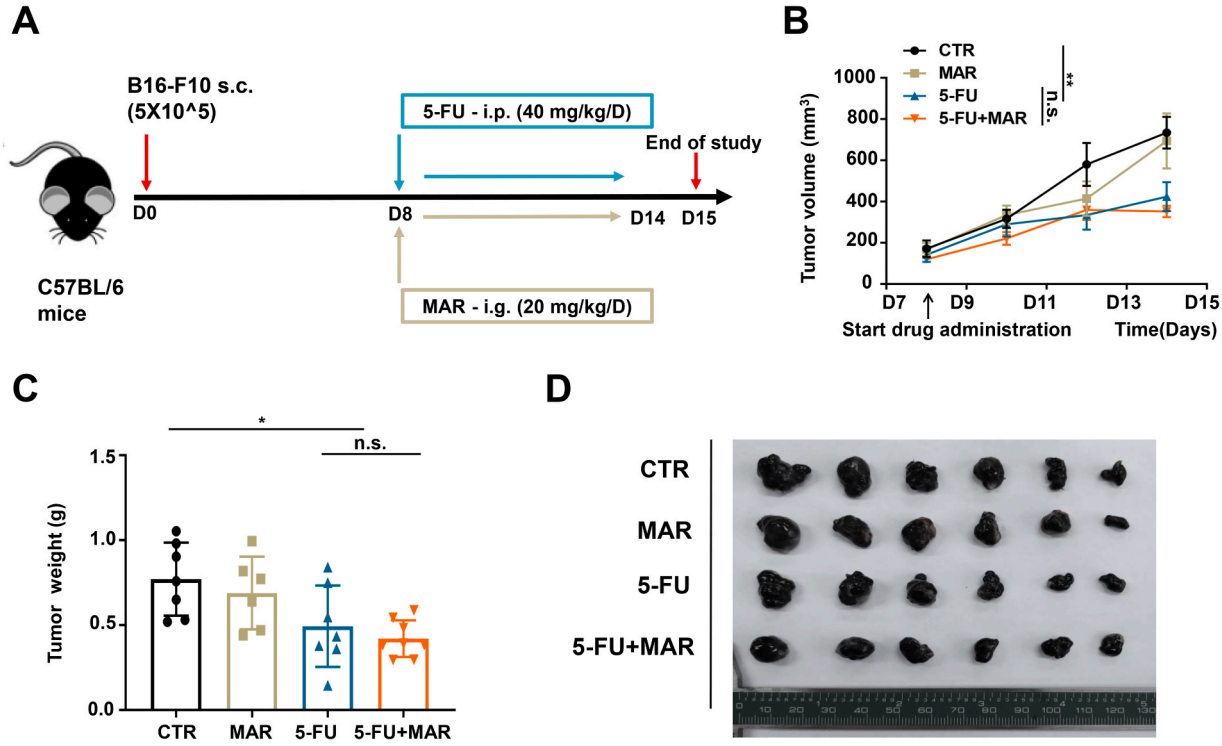

Fig. 3. Administration of MAR does not compromise the antitumor activity of 5-FU in B16-F10 tumor-bearing mice. (**A**) The schematic plot shows the setup of mouse experiments. Seven consecutive days of treatment was initiated once subcutaneous melanoma tumors reached ~200 mm^3 at day 8 post-tumor establishment. Four groups of mice were included: PBS control (CTR), 20 mg/kg/d MAR treatment only (MAR), 40 mg/kg/d 5-FU treatment only (5-FU), and combination group (5-FU + MAR). (**B**) The growth curve of tumors from indicated groups is shown. (n = 6–7). (**C**) The weight of tumors in four different treatment groups is shown. (n = 6–7). (**D**) A picture of the tumors on day 15 is shown for different groups of mice. The tumor volume data are presented as mean ± S.E.M. The growth curve was analyzed via two-way ANOVA with Bonferroni correction. The bar plots are presented as mean ± SD and the significance was calculated using a two-tailed Student's *t*-test. *P < 0.05, **P < 0.01, n.s. = no significance.

3.4. Administration of MAR restores impaired hematopoiesis in 5-FU-induced myelosuppressive mice

The antitumor effect of 5-FU usually comes with severe bone marrow damage. Hematoxylin and eosin (H&E) staining of femurs showed trabecular bone loss and bone marrow cell depletion in 5-FU-treated tumor-bearing mice (Fig. 5A and Supplementary Fig. 2A). In both models, MAR treatment attenuated 5-FU-induced bone marrow damage with the regeneration of BMCs (Fig. 5A and Supplementary Fig. 2A). Consistently, MAR treatment recovered the number of BMNCs in 5-FU-treated tumor-bearing mice (Fig. 5B and Supplementary Fig. 2B). In the B16-F10 melanoma-bearing mice, compared with the 5-FU-only treatment group, co-administration of MAR significantly increased the percentage of leukocytes (CD45+) and granulocytes (CD11b+Gr-1+) in BMCs (Fig. 5C). We further examined the effects of MAR on peripheral blood of 5-FU-treated mice by complete blood count (CBC) analysis. While 5-FU treatment dramatically reduced the number of platelets (PLT), white blood cells (WBC), and red blood cells (RBC), co-administration of MAR increased the number of WBC and PLT in peripheral blood (Fig. 5D). Collectively, by employing two tumor-bearing mouse models, we characterized the multi-lineage protective effects of MAR on the 5-FU-induced bone marrow hematopoietic injury without compromising 5-FU's antitumor activity.

3.5. Identification and functional analysis of cDEGs from in vivo mRNA-Seq data

Finally, for a better understanding of molecular changes involved in the observed MAR-mediated *in vivo* myeloprotection effect, we examined the gene expression changes of the BMNCs isolated from different treated groups of mice. The number of identified DEGs (DESeq2 P value < 0.05 and |log2FC| > 1.0) from different comparison groups was shown in Fig. 6A (Supplementary Table S2). The results suggested that there were 3,563 and 569 DEGs in 5-FU (vs CTR) and additional MAR-treated (vs 5-FU) mice, respectively. It indicates that there are remarkable changes in gene expression of BMNCs upon 5-FU and MAR treatment. We then analyzed the intersection of 3,563 DEGs in the 5-FU vs CTR group and 569 DEGs in the 5-FU + MAR vs 5-FU group. As shown in

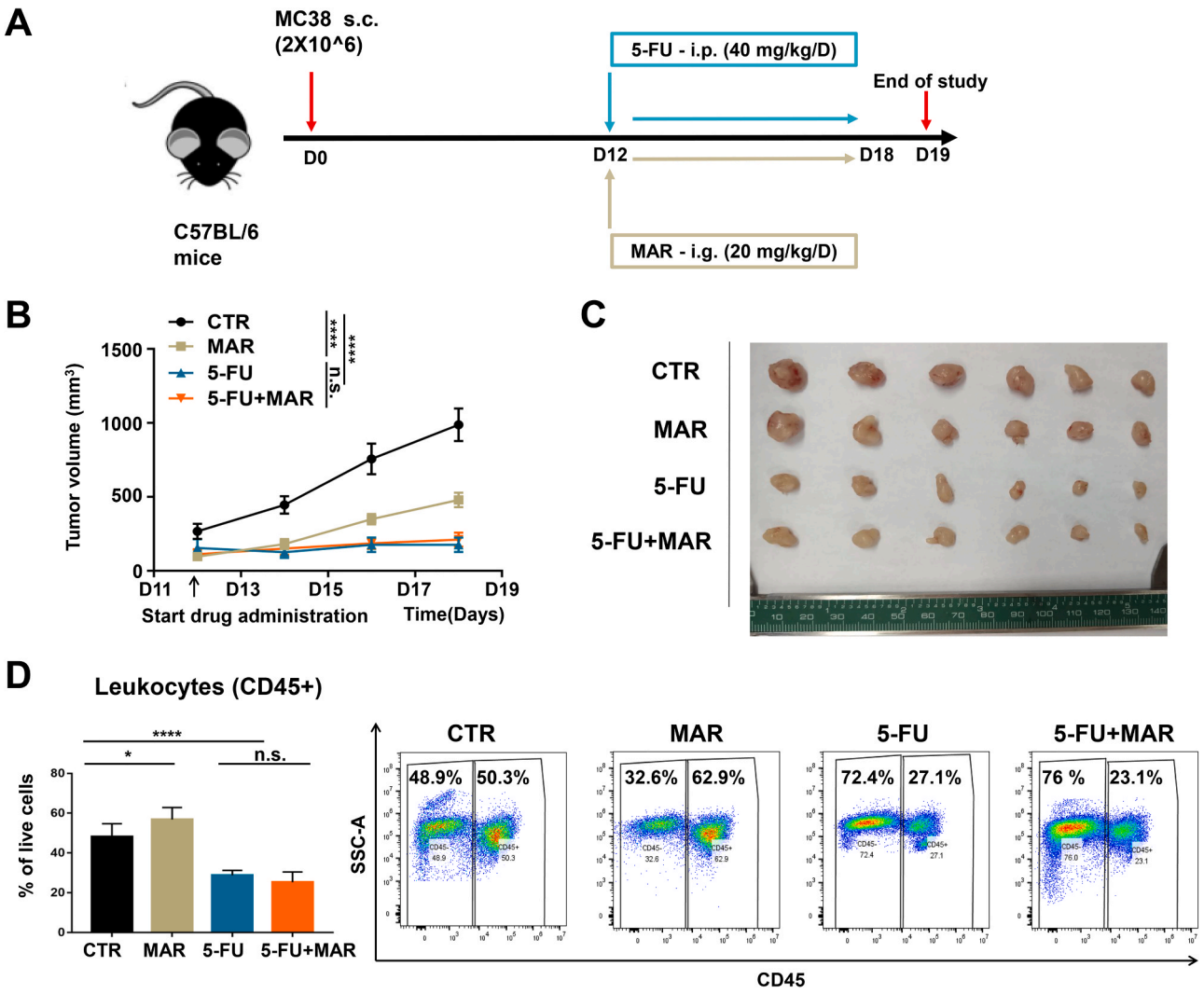

Fig. 4. Administration of MAR does not compromise the antitumor activity of 5-FU in MC38 tumor-bearing mice. (**A**) The schematic plot shows the mouse experiments setup. Seven consecutive days of treatment was initiated once subcutaneous colon tumors reached ~200 mm^3 at day 12 post-tumor establishment. Four groups of mice were included: PBS control (CTR), 20 mg/kg/d MAR treatment only (MAR), 40 mg/kg/d 5-FU treatment only (5-FU), and combination group (5-FU + MAR). (**B**) The tumor growth curve is shown. Tumor size was measured every other day. The data are expressed as mean ± S.E.M. (n = 6–7). (**C**) The picture of the tumors on day 19 is shown for different groups of mice. (**D**) MAR increases the number of leukocytes in MC38 tumor tissues. The percentage of leukocytes (CD45+) on tumor tissue from different treated mice was evaluated by flow cytometry. (n = 4–6). The tumor volume data are presented as mean ± S.E.M. The growth curve was analyzed via two-way ANOVA with Bonferroni correction. *P < 0.05, ****P < 0.0001, n.s. = no significance.

Fig. 6B, 385 cDEGs in the intersection of the above three datasets were selected for further analysis. Then, 385 cDEGs were clustered and shown as a heatmap in Fig. 6C. The expression profile in the two comparison groups showed that MAR recovered most of the cDEG expression altered by 5-FU. To further investigate the biological functions of 385 cDEGs, GO and pathway enrichment analysis were conducted (Fig. 6D). "Cell adhesion", "extracellular matrix organization", and "collagen fibril organization" were the top 3 enriched biological processes. "Proteinaceous extracellular matrix", "extracellular region", and "extracellular matrix" were the top 3 enriched cellular component terms. These molecular functions were significantly associated with heparin-binding, extracellular matrix structural constituent, and collagen binding. Besides, we found that the significantly enriched KEGG pathways of these genes were "ECM-receptor interaction", "PI3K-Akt signaling pathway", and "focal adhesion" pathways. These results indicate that MAR may modulate these pathways and biological processes, thus exhibiting multi-lineage protective effects in 5-FU-induced myelosuppressive mice.

To analyze the potential regulatory networks of these cDEGs, a PPI network of 385 cDEGs was obtained in the String database [28], including 285 nodes and 1848 edges (Fig. 7A). To identify key DEGs in the PPI network, we used the CytoHubba plugin to select the top 25 hub genes with the highest degree of connectivity for further analysis. Results showed that extracellular matrix proteins (Fn1, Fbn1, Fstl1, Lamb1, Spp1, Lamb2, Chrdl1, Cyr61 and Tnc), collagens (Col1a1, Col3a1, Col6a1, Col6a2 and Col6a3) and insulin-like growth factor-binding proteins (Igfbp3, Igfbp5 and Igfbp7) were the key nodes in the network (Fig. 7B). Furthermore, a separate enrichment analysis of GO biological process terms of these genes was performed. Top 10 terms were shown in Fig. 7C, including osteoblast differentiation, cell adhesion, regulation of cell growth, positive regulation of cell migration, wound healing, protein heterodimerization, skeletal system development, and extracellular matrix organization, etc. Using the MCODE plugin, we then provided a sub-network analysis to identify key functional clusters. The 5 most interconnected sub-networks and the top 10 enriched GO biological process terms of these sub-networks are shown in Fig. 8. In sub-network 3, only one GO term, GO: 0006508-Proteolysis, was enriched. Besides, the genes involved in sub-network 1, 2, 4, and 5 were most enriched in the collagen fibril organization, T cell

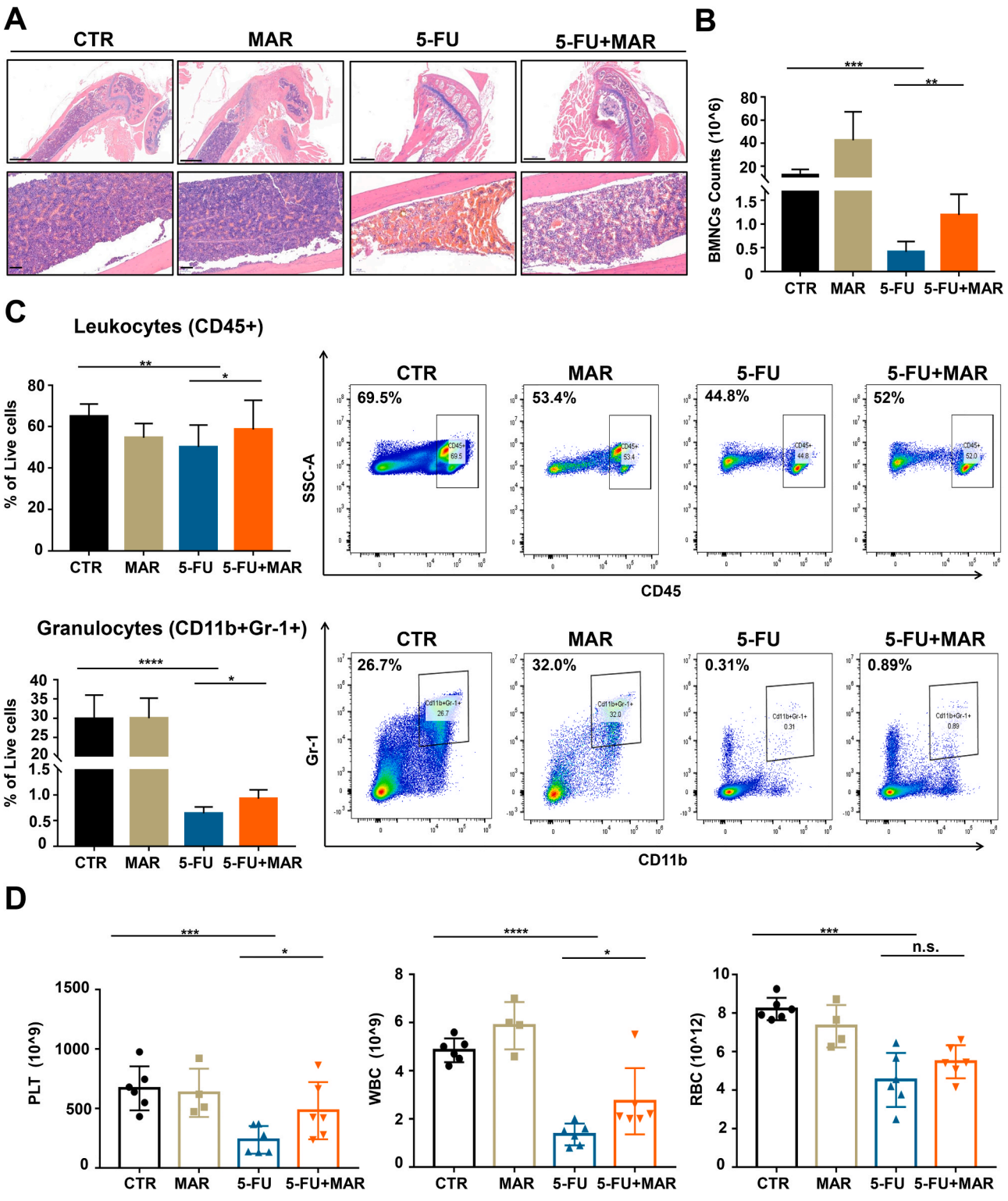

Fig. 5. Administration of MAR restores impaired hematopoiesis in B16-F10 tumor-bearing mice treated with 5-FU. (**A**) Representative H&E-stained sections of bone marrow are shown for indicated groups of mice. The scale bars in the upper and lower panel represent 500 μm and 100 μm, respectively. (**B**) MAR increases the number of BMNCs down-regulated by 5-FU. The number of BMNCs was calculated on day 15. (n = 4–6). (**C**) The protective effects of MAR on leukocyte (CD45+) and granulocytic (CD11b+Gr-1+) lineages in BMCs were evaluated by flow cytometry on day 15. (n = 4–6). (**D**) CBC analysis is performed for the peripheral blood of mice. The levels of PLT, WBC, and RBC from the indicated groups are shown. (n = 4–6). The bar plots are presented as mean ± SD and the significance was calculated using a two-tailed Student's *t*-test. *P < 0.05, **P < 0.01, ***P < 0.001, ****P < 0.0001, n.s. = no significance.

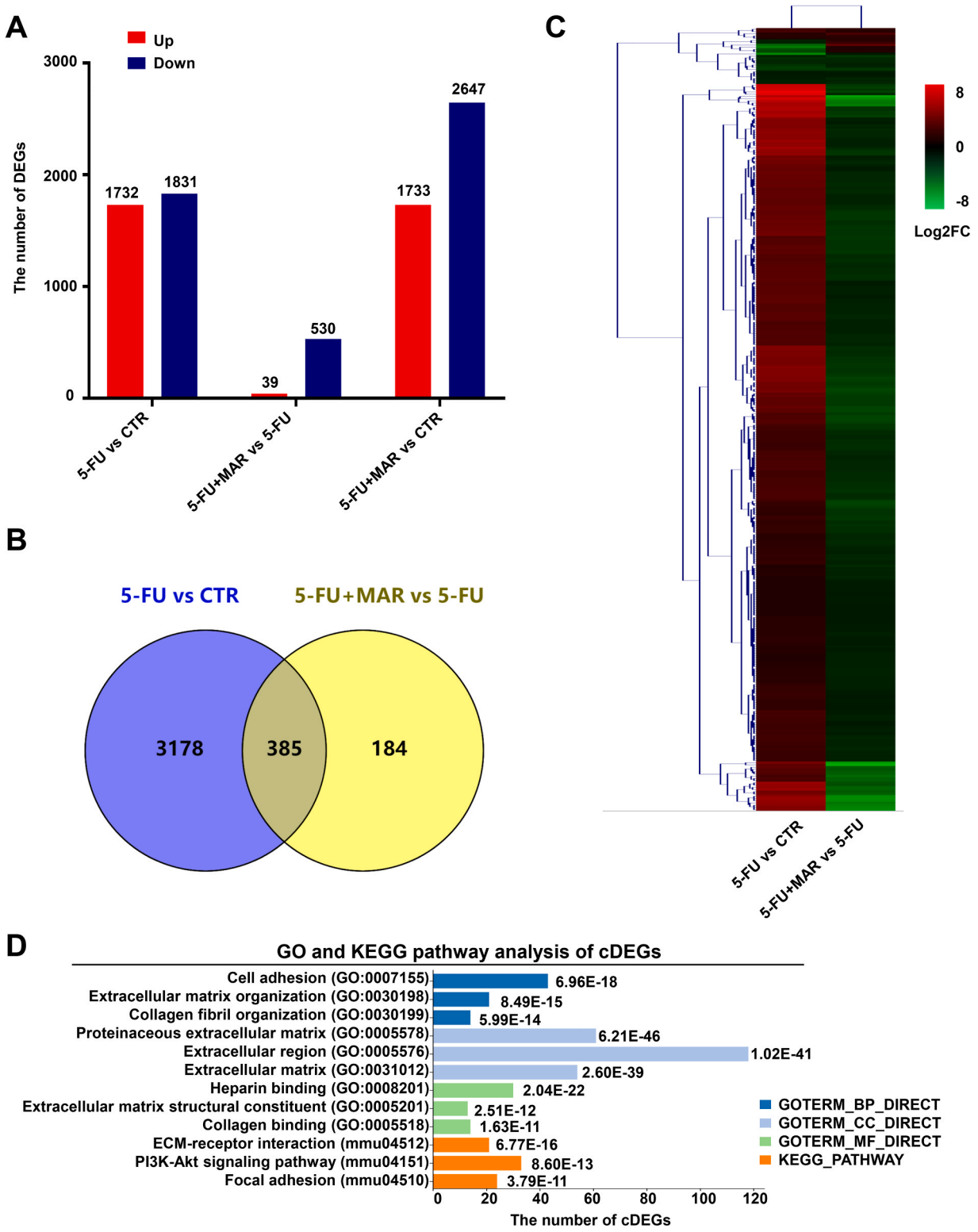

Fig. 6. cDEGs identification and functional analysis of BMNCs in the *in vivo* myelosuppression model. (**A**) Number of up- and down-regulated DEGs. (**B**) Venn diagram showing the number of commonly and uniquely DEGs in the comparison groups of 5-FU vs CTR and 5-FU + MAR vs 5-FU. 385 DEGs were co-regulated by 5-FU and MAR. (**C**) Hierarchical clustering of cDEGs. Each row depicts a gene, and each column depicts changes in each comparison group. (**D**) GO and KEGG pathway analysis of cDEGs. The top 3 terms of each category are shown. The terms are arranged by P value.

costimulation, G-protein coupled receptor signaling pathway, and response to peptide hormone, respectively. These data indicate that modulation of these biological processes may also be involved in the protective mechanism of MAR. Notably, consistent with the *ex vivo* results, *in vivo* application of MAR significantly down-regulated the apoptotic signaling pathway (sub-network 2) and inflammatory response (sub-network 4) activated by 5-FU as well (P value < 0.05).

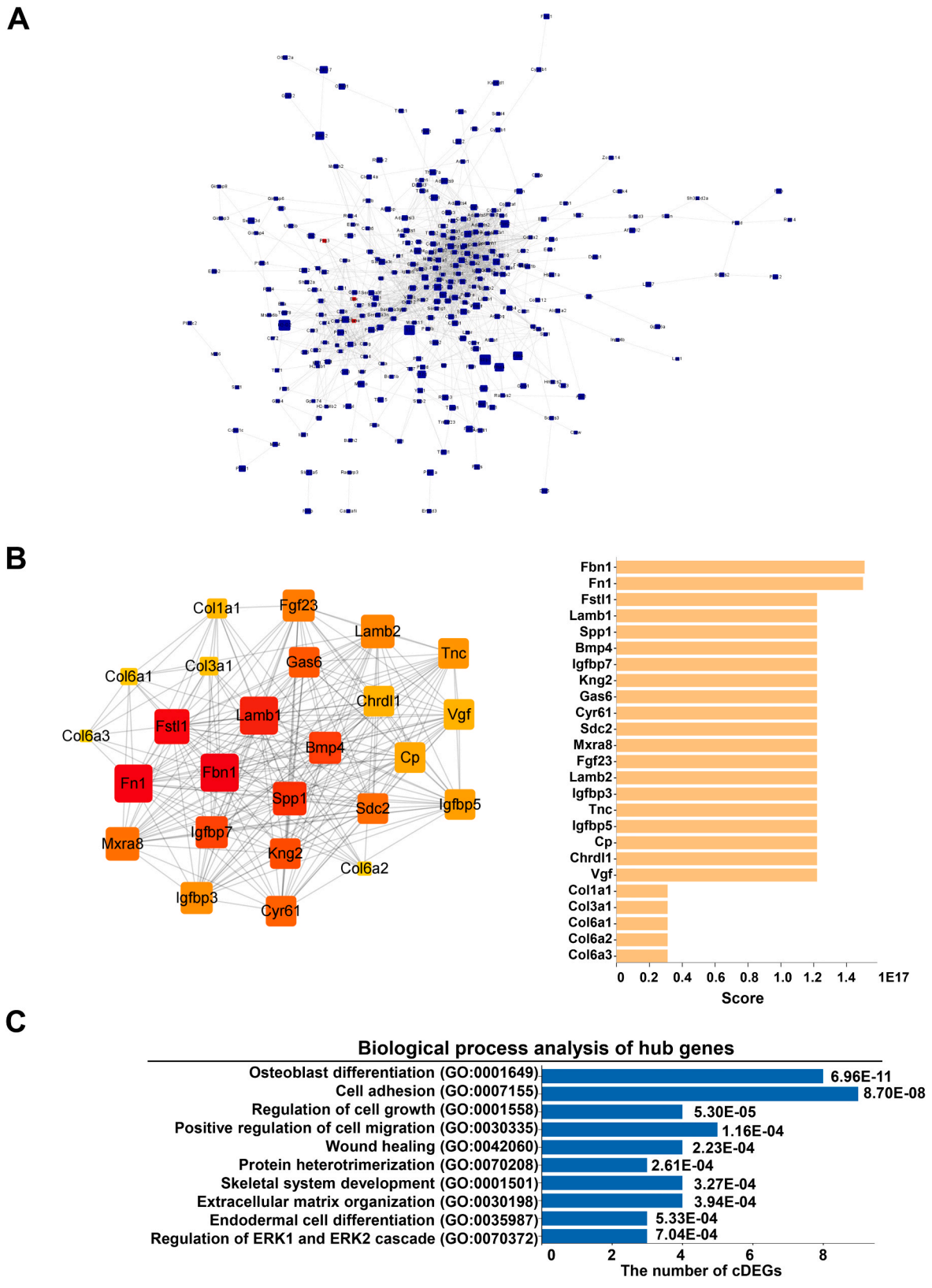

Fig. 7. PPI network analysis of cDEGs from *in vivo* mRNA-Seq data of BMNCs. (**A**) PPI network created with cDEGs associated with additional MAR. Blue nodes were down-regulated genes and red nodes were up-regulated genes by MAR, respectively. (**B**) PPI network analysis of the top 25 hub genes. Large and warm color nodes share higher connectivity degrees. The order of genes is ranked in the order of connectivity score from high to low. (**C**) GO biological process enrichment analysis of the top 25 hub genes. The GO terms are arranged by P value. (For interpretation of the references to colour in this figure legend, the reader is referred to the web version of this article.)

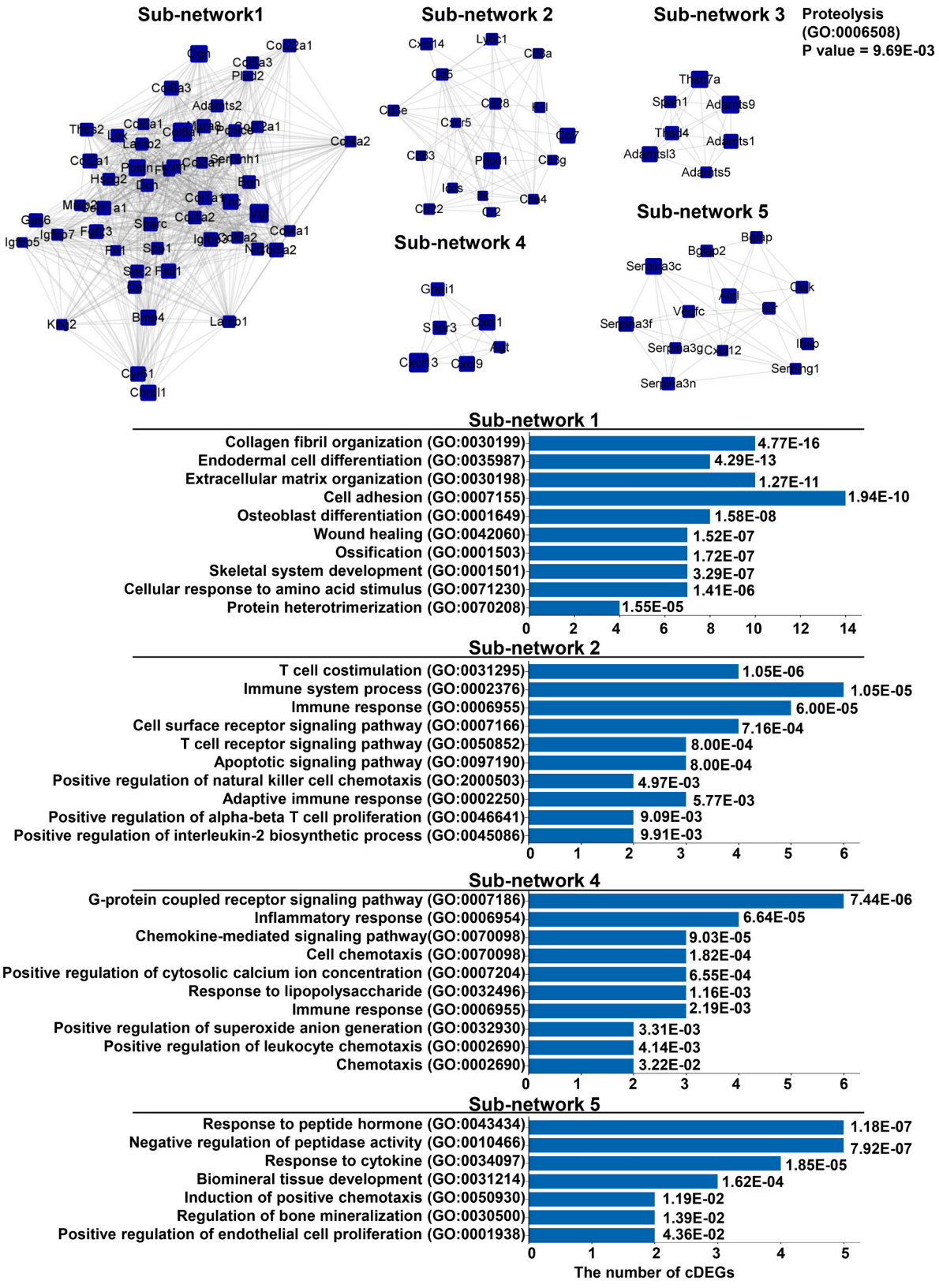

Fig. 8. Sub-network analysis of cDEGs from *in vivo* mRNA-Seq data. Best 5 interconnected sub-networks and GO biological process enrichment analysis for these sub-networks. Sub-network 1 (score = 27.837) was constructed with 50 nodes and 682 edges. Sub-network 2 (score = 8.250) was constructed with 17 nodes and 66 edges. Sub-network 3 (score = 7.000) was constructed with 7 nodes and 21 edges. Sub-network 4 (score = 6.000) was constructed with 6 nodes and 15 edges. Sub-network 5 (score = 5.833) was constructed with 13 nodes and 25 edges. Blue nodes represent down-regulated genes with additional MAR, and the size of each node represents the absolute value of log2FC. The GO terms are arranged by P value. (For interpretation of the references to colour in this figure legend, the reader is referred to the web version of this article.)

3.6. MAR reduces the inflammation-related gene expression elevated by 5-FU

To further investigate the effects of MAR on 5-FU-induced bone marrow inflammation, we selected 6 inflammation-related hub genes (Il1b, Tlr2, Relb, Cxcl2, Cyr61, and Tnc) and verified their mRNA expression levels by RT-qPCR. The fragments per kilobase million (FPKM) values of these genes were shown in Fig. 9A and B (left panel). After exposure to 5-FU, the expression of Il1b, Tlr2, Relb, and Cxcl2 in BMSCs was significantly increased. Meanwhile, additional MAR significantly reduced the mRMA levels of these genes (Fig. 9A, right panel). In 5-FU-induced myelosuppressive mice, the expression of secreted extracellular matrix molecule Cyr61 and extracellular matrix glycoprotein Tnc was significantly elevated and MAR co-administration significantly down-regulated their expression levels (Fig. 9B, right panel). These results suggest that MAR is most likely to be involved in the regulation of inflammatory response in the hematopoietic microenvironment to improve 5-FU-impaired hematopoietic function. Besides, these genes showed similar mRNA expression patterns in transcriptomic and RT-qPCR analysis, indicating the reliability of the mRNA-Seq data.

4. Discussion

In China, a variety of *Rehmannia glutinosa*-included traditional Chinese medicine formulas have been frequently prescribed for treating chemotherapy-induced pancytopenia. In this study, we described the protective effects of MAR, the active ingredient found in *Rehmannia glutinosa*, on 5-FU-induced bone marrow cytotoxicity and characterized its impact on the antitumor effect of 5-FU. Besides, based on the *ex vivo* and *in vivo* transcriptomic analysis, we revealed the MAR's associated biological processes, signaling pathways, and pivot genes.

MAR has been reported with several pharmacological properties, including anti-sports anemia [23], estrogenic/antiestrogenic properties [33], and reduction of skeletal muscle fatigue [34]. Previously, we found that MAR could facilitate the proliferation of HSCs in 5-FU-induced myelosuppressive mice , both *ex vivo* and *in vivo* [19,22]. In this study, we further focus on the effects of MAR in BMSCs, the physiological microenvironment in bone marrow, to provide a more comprehensive analysis of MAR's hematopoietic activity.

BMNCs are composed of HSCs and BMSCs [35]. Located in the bone marrow stroma, BMSCs are a group of pluripotent stem cells and can generate osteocytes, adipocytes, endothelial cells, and fibroblasts, which constitute most of the hematopoietic microenvironment and are

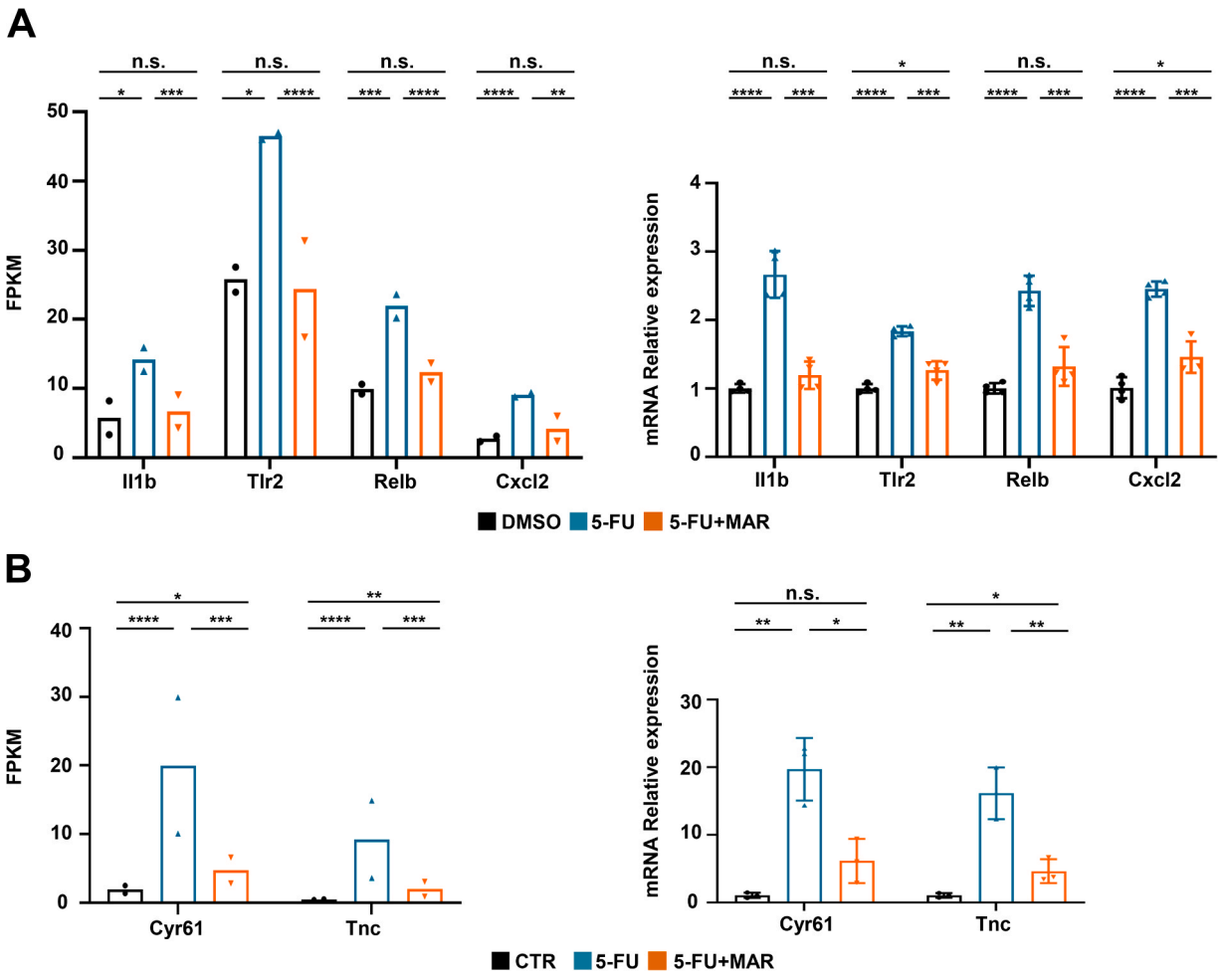

Fig. 9. Verification of inflammation-related gene expression using RT-qPCR. (**A**) RT-qPCR was applied to verify the relative expression of inflammation-related hub genes obtained from *ex vivo* transcriptomic data of BMSCs. The FPKM values from the mRNA-Seq analysis are shown in the left panel, two dots represent the two biological replicates and the bar represents the average. mRNA expression levels of these genes were evaluated by RT-qPCR in BMSCs exposed to indicated conditions for 48 h (right). (n = 4). (**B**) RT-qPCR was applied to verify the relative expression of inflammation-related hub genes obtained from *in vivo* transcriptomic data of BMNCs. The FPKM values from the mRNA-Seq analysis are shown in the left panel, two dots represent the two biological replicates and the bar represents the average. mRNA expression levels of these genes were evaluated by RT-qPCR in BMNCs obtained from different treatment groups (right). (n = 3). Data are shown as mean ± SD. *P < 0.05, **P < 0.01, ***P < 0.001, *** *P < 0.0001, n.s. = no significance.

essential for maintaining hematopoietic function [36]. It has been reported that even after receiving sufficient application of HSCs, patients that received high-dose chemotherapy may still have abnormal peripheral blood counts [37], suggesting that hematopoietic microenvironment damage induced by chemotherapy may affect the bone marrow hematopoietic reconstruction. Besides, it was well-demonstrated that chemo-drugs could cause bone marrow stromal cell injury, of which apoptosis is the main form of damage [38].

In this study, we established an *ex vivo* 5-FU-induced bone marrow stromal cell injury model and demonstrated that MAR interfered with 5-FU-induced apoptosis in BMSCs. The corresponding transcriptome and RT-qPCR analysis revealed that MAR significantly down-regulated the expression of inflammation-related genes elevated by 5-FU, including key regulatory pro-inflammatory genes Il1b, Tlr2, Relb, and Cxcl2. In line with a previous study, 5-FU had an inhibitory effect on BMSCs growth and increased the secretion of inflammatory factors [39]. Besides, the oppositely down-regulated cDEGs by MAR were mostly enriched in the TNF signaling pathway. Consistently, MAR up-regulated the GO biological process of negative regulation of tumor necrosis factor production. It is well-known that the TNF signaling pathway is closely related to cell apoptosis, survival, and inflammation. Therefore, these results indicate that MAR may attenuate 5-FU-induced bone marrow stromal cell injury through the TNF pathway, thereby inhibiting inflammation response and apoptosis, ultimately promoting hematopoietic function.

In B16-F10 and MC38 tumor-bearing mice, we first determined that MAR did not interfere with the antitumor effect of 5-FU, providing evidence for its further clinical application. Besides, in our *in vivo* 5-FU-induced myelosuppression mouse model, we applied continuous application of 5-FU to achieve a degree of neutropenia similar to that seen in some cancer patients treated with 5-FU [24]. It is worth noting that the *in vivo* chemoprotective activity of MAR in the hematopoietic system is impressive. As reported, the characteristics of 5-FU-induced bone marrow damage are the loss of BMNCs and the decrease of circulatory WBC [40]. The BMNCs count in the bone marrow is a direct reflection of the bone marrow health state [41]. We found that the total number of BMNCs was significantly reduced after 5-FU treatment with apparent bone marrow pathological damage, indicating the state of bone marrow suppression. Compared with the 5-FU-only treatment group, the additional MAR significantly increased the count of BMNCs in the bone marrow accompanied by the recovery of peripheral WBC and PLT counts, indicating its clinical therapeutic potential. Furthermore, we provided evidence that MAR increased the percentage of leukocytes (CD45+) and granulocytes (CD11b+Gr-1+) in the bone marrow. These results suggest that MAR possesses a broad relief activity on multi-lineage myelosuppression, potentially overcoming the limitations of current treatment strategies, such as the transfusion of blood cell components and the administration of growth factors.

Mechanistically, the bone marrow toxicity of 5-FU may be related to the increased bone marrow inflammation, osteoclast formation, and accelerated bone loss [42]. Notably, the most enriched pathways of cDEGs include ECM-receptor interaction and focal adhesion. Besides, we found a group of associated hub cDEGs, including multiple extracellular matrix glycoproteins and collagen genes, were oppositely altered upon 5-FU and MAR administration, such as Cyr61 and Tnc. It has been reported that ECM is composed of collagen, proteoglycan, and glycoprotein, which is an indispensable component for maintaining the function and structure of the bone hematopoietic microenvironment [43]. Our results indicate that MAR may improve hematopoietic function by regulating extracellular matrix organization interfered by 5-FU. Previous studies have shown that the destruction of ECM and adhesion junctions may promote the development of inflammation-related diseases [44]. Consistently, we found that 5-FU significantly induced the expression of several pro-inflammatory related genes, including Fstl1, Spp1, Gas6, Cyr61, and Tnc [45–49]. Fstl1 is a novel pro-inflammatory cytokine and positively correlated with the severity of many arthritic diseases [46]. Spp1 not only acts as a component of the extracellular matrix but also exists as a soluble cytokine that is often up-regulated during inflammation [45]. Gas6 and Cyr61 have been reported to promote inflammation, and the silencing of Tnc may relieve apoptosis and inflammation response [48–50]. As previously reported, the inflammatory activity may lead to the disorder of the bone marrow microenvironment and produce obvious harmful effects to the hematopoietic system [51]. In 5-FU-induced myelosuppressive mice, we found that *in vivo* administration of MAR significantly reduced the expression of these pro-inflammatory genes increased by 5-FU, especially Cyr61 and Tnc. In line with *ex vivo* results of BMSCs, this evidence strongly supported that MAR might restore the hematopoietic function by inhibiting inflammation in the hematopoietic microenvironment.

On the other hand, we found that 25 hub genes oppositely down-regulated by MAR were most enriched in the osteoblast differentiation process, including Chrdl1 and insulin-like growth factor-binding proteins (Igfbp3, Igfbp5, and Igfbp7). These genes are important regulators of osteoclast formation and bone metabolism, which is closely related to the bone marrow microenvironment [52–55]. According to a previous report, 5-FU might accelerate bone loss by inducing excessive differentiation of osteoclasts [56]. Therefore, it is likely that MAR may suppress the excessive differentiation of osteoclasts to maintain the bone marrow microenvironment. Collectively, our results suggest that MAR may restore the bone marrow microenvironment to improve hematopoietic function by regulating extracellular matrix organization, suppressing 5-FU-induced inflammation, osteoblast differentiation, and bone loss. One of the other most enriched pathways was the PI3K-Akt signaling pathway. Previous studies have shown that excessive PI3K-Akt activation may lead to the depletion of HSCs [57]. Therefore, MAR may inhibit the overactive PI3K/Akt signaling pathway induced by 5-FU, thereby increasing the survival of HSCs to improve hematopoietic function.

In summary, we proposed a multi-pathway therapeutic mechanism model of MAR and highlighted its regulatory role in the inflammation response of the hematopoietic microenvironment. These results provide a theoretical basis for the further development and clinical application of MAR. To further reveal the potential mechanism of MAR, future work may involve the validation of the associated biological processes aforementioned.

5. Conclusion

MAR alleviates bone marrow injury and exhibits multi-lineage protective effects in 5-FU-induced myelosuppressive mice without compromising its antitumor activity. Its molecular mechanism may be related to the increased survival of BMNCs and the improvement of the bone marrow microenvironment by regulating extracellular matrix organization, inhibiting osteoblast differentiation and inflammation response, and reducing cell apoptosis. We highlighted the critical role of inflammation-related genes upon 5-FU and MAR treatment, including Il1b, Tlr2, Relb, Cxcl2, Cyr61, and Tnc. Our findings provide a framework for the continuous study of MAR and a theoretical basis for the clinical usage of *Rehmannia glutinosa*.

Conflict of interest statement

All authors declare that they have no known competing financial interests or personal relationships that could inappropriately influence the work reported in this study.

Acknowledgment

This study was funded by a grant from the Science and Technology Department of Zhejiang Province, China (No. 2019C03018) and a grant from Shandong Dong-E E-Jiao Co. Ltd (No. 520003-I21902).

Appendix A. Supporting information

Supplementary data associated with this article can be found in the online version at doi:10.1016/j.biopha.2021.111501.

References

[1] D.B. Longley, D.P. Harkin, P.G. Johnston, 5-fluorouracil: mechanisms of action and clinical strategies, Nat. Rev. Cancer 3 (2003) 330–338.
[2] C. Isanbor, D. O'Hagan, Fluorine in medicinal chemistry: a review of anti-cancer agents, J. Fluor. Chem. 127 (2006) 303–319.
[3] J. Kærn, C. Tropé, V. Abeler, T. Iversen, K. Kjørstad, A phase II study of 5-fluorouracil/cisplatinum in recurrent cervical cancer, Acta Oncol. 29 (1990) 25–28, https://doi.org/10.3109/02841869009089987.
[4] R.L. Schilsky, J. Hohneker, M.J. Ratain, L. Janisch, L. Smetzer, V.S. Lucas, S. P. Khor, R. Diasio, D.D. Von Hoff, H.A. Burris 3rd, Phase I clinical and pharmacologic study of eniluracil plus fluorouracil in patients with advanced cancer. J. Clin. Oncol. Off. J. Am. Soc. Clin. Oncol. 16 (1998) 1450–1457, https://doi.org/10.1200/JCO.1998.16.4.1450.
[5] C. Veeresham, Natural products derived from plants as a source of drugs, (2012).
[6] A.F. Wali, S. Majid, S. Rasool, S.B. Shehada, S.K. Abdulkareem, A. Firdous, S. Beigh, S. Shakeel, S. Mushtaq, I. Akbar, H. Madhkali, M.U. Rehman, Natural products against cancer: review on phytochemicals from marine sources in preventing cancer, Saudi Pharm. J. 27 (2019) 767–777.
[7] Q.-Y. Zhang, F.-X. Wang, K.-K. Jia, L.-D. Kong, Natural product interventions for chemotherapy and radiotherapy-induced side effects, Front. Pharmacol. 9 (2018) 1253, https://doi.org/10.3389/fphar.2018.01253.
[8] X. Chen, J. Wang, Z. Fu, B. Zhu, J. Wang, S. Guan, Z. Hua, Curcumin activates DNA repair pathway in bone marrow to improve carboplatin-induced myelosuppression, Sci. Rep. 7 (2017) 17724.
[9] S. Wang, G. Zheng, S. Tian, Y. Zhang, L. Shen, Y. Pak, Y. Shen, J. Qian, Echinacoside improves hematopoietic function in 5-FU-induced myelosuppression mice, Life Sci. 123 (2015) 86–92.
[10] J. Gu, Treatment of Fufang Ejiao Syrup for 37 cases of anaemia, World Chin. Med. (2012).
[11] J.N. Barreto, K.B. McCullough, L.L. Ice, J.A. Smith, Antineoplastic agents and the associated myelosuppressive effects: a review, J. Pharm. Pract. 27 (2014) 440–446.
[12] J.X. Chen, X.H. Shen, Effects of qisheng mixture on chemotherapy induced myelosuppression in patients with colorectal cancer, Zhongguo Zhong Xi Yi Jie He Za Zhi Zhongguo Zhongxiyi Jiehe Zazhi Chin. J. Integr. Tradit. West. Med. 32 (2012) 1161–1165.
[13] J. Hong, X. Chen, J. Huang, C. Li, L. Zhong, L. Chen, J. Wu, O. Huang, J. He, L. Zhu, Danggui Buxue decoction, a classical formula of traditional Chinese medicine, fails to prevent myelosuppression in breast cancer patients treated with adjuvant chemotherapy: a prospective study, Integr. Cancer Ther. 16 (2017) 406–413.
[14] Z. Wei, X. Fang, M. Miao, The analysis of the adverse reaction of traditional Chinese medicine tumor bone marrow suppression, IOP Conf. Ser. Mater. Sci. Eng. 301 (2018), 012065, https://doi.org/10.1088/1757-899X/301/1/012065.
[15] J. Liu, M. Pei, C. Zheng, Y. Li, Y. Wang, A. Lu, L. Yang, A Systems-Pharmacology Analysis of Herbal Medicines.pdf, (2013).
[16] C. Gao, L. Yang, M. Chen, H. Zhang, Principles of differentiation and prescription for vitiligo in traditional Chinese medicine based on a literature investigation, Integr. Med. Int. 2 (2015) 149–156, https://doi.org/10.1159/000441845.
[17] A. Kolasani, H. Xu, M. Millikan, Determination and comparison of mineral elements in traditional Chinese herbal formulae at different decoction times used to improve kidney function - chemometric approach, Afr. J. Tradit. Complement. Altern. Med. 8 (2011) 191–197, https://doi.org/10.4314/ajtcam.v8i5S.25.
[18] Y. Wu, Q. Wan, L. Shi, J. Ou, Y.Q. Li, F. He, H. Wang, J. Gao, Siwu granules and erythropoietin synergistically ameliorated anemia in adenine-induced chronic renal failure rats, evidence-based complement, Altern. Med. 2019 (2019), https://doi.org/10.1155/2019/5832105.
[19] L. Shen, H. Chen, Q. Zhu, Y. Wang, S. Wang, J. Qian, Y. Wang, H. Qu, Identification of bioactive ingredients with immuno-enhancement and anti-oxidative effects from Fufang-Ejiao-Syrup by LC–MSn combined with bioassays, J. Pharm. Biomed. Anal. 117 (2016) 363–371.
[20] X. Li, M. Zhou, P. Shen, J. Zhang, C. Chu, Z. Ge, J. Yan, [Chemical constituents from Rehmannia glutinosa], Zhongguo Zhong Yao Za Zhi Zhongguo Zhongyao Zazhi China J. Chin. Mater. Med. 36 (2011) 3125–3129.
[21] Y.F. Liu, D. Liang, H. Luo, Z.Y. Hao, Y. Wang, C.L. Zhang, R.Y. Chen, D.Q. Yu, Chemical constituents from root tubers of Rehmannia glutinosa, China Tradit. Herb. Drugs 45 (16) (2014) 22 (2014).
[22] X. Li, Y. Zhang, Z. Hong, S. Gong, W. Liu, X. Zhou, Y. Sun, J. Qian, H. Qu, Transcriptome profiling analysis reveals the potential mechanisms of three bioactive ingredients of Fufang E'jiao Jiang during chemotherapy-induced myelosuppression in mice, Front. Pharmacol. 9 (2018).
[23] M. Zhu, N. Tan, H. Zhu, G. Zeng, W. He, B. Yu, X. Chen, Anti-sports anaemia effects of verbascoside and martynoside in mice, Int. J. Sports Med. 31 (2010) 537–541.
[24] A. Lindner, D. Santilli, J. Hodgett, C. Nerlinger, Effects of 5-fluorouracil on the hematopoietic system of the mouse, Cancer Res. 20 (1960) 497–502.
[25] D.W. Huang, B.T. Sherman, R.A. Lempicki, Bioinformatics enrichment tools: paths toward the comprehensive functional analysis of large gene lists, Nucleic Acids Res. 37 (2009) 1–13.
[26] D.W. Huang, B.T. Sherman, R.A. Lempicki, Systematic and integrative analysis of large gene lists using DAVID bioinformatics resources, Nat. Protoc. 4 (2009) 44–57.
[27] P. Shannon, A. Markiel, O. Ozier, N.S. Baliga, J.T. Wang, D. Ramage, N. Amin, B. Schwikowski, T. Ideker, Cytoscape: a software environment for integrated models of biomolecular interaction networks, Genome Res. 13 (2003) 2498–2504.
[28] D. Szklarczyk, A.L. Gable, D. Lyon, A. Junge, S. Wyder, J. Huerta-Cepas, M. Simonovic, N.T. Doncheva, J.H. Morris, P. Bork, L.J. Jensen, C. Mering, STRING v11: protein–protein association networks with increased coverage, supporting functional discovery in genome-wide experimental datasets, Nucleic Acids Res. 47 (2019) D607–D613.
[29] C.-H. Chin, S.-H. Chen, H.-H. Wu, C.-W. Ho, M.-T. Ko, C.-Y. Lin, cytoHubba: identifying hub objects and sub-networks from complex interactome, BMC Syst. Biol. 8 (2014) S11.
[30] G.D. Bader, C.W.V. Hogue, An automated method for finding molecular complexes in large protein interaction networks, BMC Bioinforma. 4 (2003) 2.
[31] C.J. Van Groeningen, G.J. Peters, H.M. Pinedo, -induced toxicity by oral administration of reversal of 5-fluorouraciluridine, Ann. Oncol. 4 (1993) 317–320.
[32] G.J. Peters, J. van Dijk, E. Laurensse, C.J. van Groeningen, J. Lankelma, A. Leyva, J.C. Nadal, H.M. Pinedo, In vitro biochemical and in vivo biological studies of the uridine "rescue" of 5-fluorouracil, Br. J. Cancer 57 (1988) 259–265, https://doi.org/10.1038/bjc.1988.56.
[33] Z. Papoutsi, E. Kassi, S. Mitakou, N. Aligiannis, A. Tsiapara, G.P. Chrousos, P. Moutsatsou, Acteoside and martynoside exhibit estrogenic/antiestrogenic properties, J. Steroid Biochem. Mol. Biol. 98 (2006) 63–71, https://doi.org/10.1016/J.JSBMB.2005.07.005.
[34] F. Liao, R.L. Zheng, J.J. Gao, Z.J. Jia, Retardation of skeletal muscle fatigue by the two phenylpropanoid glycosides: verbascoside and martynoside from Pedicularis plicata Maxim, Phyther. Res. Int. J. Devoted Pharmacol. Toxicol. Eval. Nat. Prod. Deriv. 13 (1999) 621–623.
[35] E.L. Herzog, L. Chai, D.S. Krause, Plasticity of marrow-derived stem cells, Blood 102 (2003) 3483–3493.
[36] A. Friedenstein, Stromal-hematopoietic interrelationships: Maximov's ideas and modern models, in: Mod. Trends Hum. Leuk. VIII, Springer, 1989, pp. 159–167.
[37] J. Domenech, F. Roingeard, C. Binet, The mechanisms involved in the impairment of hematopoiesis after autologous bone marrow transplantation, Leuk. Lymphoma 24 (1997) 239–256.
[38] W. Jin-huan, W. Zhen-ling, W. Xiao-fang, Z. Zhi-gang, Damage of chemotherapy agents to bone marrow mesenchymal stem cells, Chinese, J. Tissue Eng. Res. 18 (2014) 8080.
[39] H. Xiao, L. Xiong, X. Song, P. Jin, L. Chen, X. Chen, H. Yao, Y. Wang, L. Wang, Angelica sinensis polysaccharides ameliorate stress-induced premature senescence of hematopoietic cell via protecting bone marrow stromal cells from oxidative injuries caused by 5-fluorouracil, IJMS 18 (2017) 2265.
[40] K. Shitara, K. Matsuo, D. Takahari, T. Yokota, Y. Inaba, H. Yamaura, Y. Sato, M. Najima, T. Ura, K. Muro, Neutropaenia as a prognostic factor in metastatic colorectal cancer patients undergoing chemotherapy with first-line FOLFOX, Eur. J. Cancer 45 (2009) 1757–1763.
[41] P.J. Carey, Drug-induced myelosuppression, Drug Saf. 26 (2003) 691–706.
[42] R. Raghu Nadhanan, S.M. Abimosleh, Y.-W. Su, M.A. Scherer, G.S. Howarth, C. J. Xian, Dietary emu oil supplementation suppresses 5-fluorouracil chemotherapy-induced inflammation, osteoclast formation, and bone loss, Am. J. Physiol. Metab. 302 (2012) E1440–E1449.
[43] X. Lin, S. Patil, Y.-G. Gao, A. Qian, The bone extracellular matrix in bone formation and regeneration, Front. Pharmacol. 11 (2020).
[44] C. Bonnans, J. Chou, Z. Werb, Remodelling the extracellular matrix in development and disease, Nat. Rev. Mol. Cell Biol. 15 (2014) 786–801.
[45] S.A. Lund, C.M. Giachelli, M. Scatena, The role of osteopontin in inflammatory processes, J. Cell Commun. Signal. 3 (2009) 311–322.
[46] Y. Chaly, A.D. Marinov, L. Oxburgh, D.S. Bushnell, R. Hirsch, FSTL1 promotes arthritis in mice by enhancing inflammatory cytokine/chemokine expression, Arthritis Rheum. 64 (2012) 1082–1088.
[47] X. Zhu, L. Xiao, R. Huo, J. Zhang, J. Lin, J. Xie, S. Sun, Y. He, Y. Sun, Z. Zhou, B. Shen, N. Li, Cyr61 is involved in neutrophil infiltration in joints by inducing IL-8 production by fibroblast-like synoviocytes in rheumatoid arthritis, Arthritis Res. Ther. 15 (2013) 1–14.
[48] M. Zhou, K. Ze, L. Hua, L. Liu, L. Kuai, M. Zhang, B. Li, Y. Wang, X. Li, Cyr61 promotes inflammation of a Gouty arthritis model in rats, Mediat. Inflamm. 2020 (2020) 1–13.
[49] M. Tjwa, L. Bellido-Martin, Y. Lin, E. Lutgens, S. Plaisance, F. Bono, N. Delesque-Touchard, C. Hervé, R. Moura, A.D. Billiau, C. Aparicio, M. Levi, M. Daemen, M. Dewerchin, F. Lupu, J. Arnout, J.M. Herbert, M. Waer, P. García de Frutos, B. Dahlbäck, P. Carmeliet, M.F. Hoylaerts, L. Moons, Gas6 promotes inflammation by enhancing interactions between endothelial cells, platelets, and leukocytes, Blood J. Am. Soc. Hematol. 111 (2008) 4096–4105.
[50] X. Tong, J. Zhang, M. Shen, J. Zhang, Silencing of Tenascin-C inhibited inflammation and apoptosis via PI3K/Akt/NF-κB signaling pathway in subarachnoid hemorrhage cell model. J. Stroke Cerebrovasc. Dis. 29 (2020), 104485 https://doi.org/10.1016/j.jstrokecerebrovasdis.2019.104485.
[51] H. Takizawa, M.G. Manz, Impact of inflammation on early hematopoiesis and the microenvironment, Int. J. Hematol. 106 (2017) 27–33.
[52] W. Zhang, E. Chen, M. Chen, C. Ye, Y. Qi, Q. Ding, H. Li, D. Xue, X. Gao, Z. Pan, IGFBP7 regulates the osteogenic differentiation of bone marrow-derived mesenchymal stem cells via Wnt/$β$-catenin signaling pathway, FASEB J. 32 (2018) 2280–2291.
[53] K. Eguchi, Y. Akiba, N. Akiba, M. Nagasawa, L.F. Cooper, K. Uoshima, Insulin-like growth factor binding Protein-3 suppresses osteoblast differentiation via bone morphogenetic protein-2, Biochem. Biophys. Res. Commun. 507 (2018) 465–470.

[54] A. Mukherjee, P. Rotwein, Insulin-like growth factor-binding protein-5 inhibits osteoblast differentiation and skeletal growth by blocking insulin-like growth factor actions, Mol. Endocrinol. 22 (2008) 1238–1250.

[55] T. Liu, B. Li, X.-F. Zheng, S.-D. Jiang, Z.-Z. Zhou, W.-N. Xu, H.-L. Zheng, C.-D. Wang, X.-L. Zhang, L.-S. Jiang, Chordin-like 1 improves osteogenesis of bone marrow mesenchymal stem cells through enhancing BMP4-SMAD pathway, Front. Endocrinol. 10 (2019) 360, https://doi.org/10.3389/fendo.2019.00360.

[56] J.M. Quach, M. Askmyr, T. Jovic, E.K. Baker, N.C. Walsh, S.J. Harrison, P. Neeson, D. Ritchie, P.R. Ebeling, L.E. Purton, Myelosuppressive therapies significantly increase pro-inflammatory cytokines and directly cause bone loss, J. Bone Miner. Res. 30 (2015) 886–897.

[57] M.G. Kharas, R. Okabe, J.J. Ganis, M. Gozo, T. Khandan, M. Paktinat, D. G. Gilliland, K. Gritsman, Constitutively active AKT depletes hematopoietic stem cells and induces leukemia in mice, Blood J. Am. Soc. Hematol. 115 (2010) 1406–1415.